

Photoluminescence and acceptor level state of *p*-type nitrogen-doped MgZnO films

Z.P. Wei

Key Laboratory of Excited State Processes, Changchun Institute of Optics, Fine Mechanics and Physics, Chinese Academy of Sciences, Changchun 130033, China; Graduate School of Chinese Academy of Sciences, Beijing 100039, China; and Department of Physics, Changchun University of Science and Technology, Changchun 130022, China

B. Yao,^{a)} X.H. Wang, Z.Z. Zhang, Y.M. Lu, D.Z. Shen, B.H. Li, J.Y. Zhang, D.X. Zhao, and X.W. Fan

Key Laboratory of Excited State Processes, Changchun Institute of Optics, Fine Mechanics and Physics, Chinese Academy of Sciences, Changchun 130033, China

Z.K. Tang

Department of Physics, Hong Kong University of Science & Technology, Clear Water Bay, Kowloon, Hong Kong, China

(Received 3 April 2007; accepted 1 June 2007)

A wurtzite nitrogen-doped MgZnO (MgZnO:N) film was grown by plasma-assisted molecular-beam epitaxy (PAMBE) on *c*-plane sapphire using radical NO as oxygen source and nitrogen dopant. The as-grown film shows *n*-type conduction at room temperature, but transforms into *p*-type conduction after annealed. Photoluminescence (PL) spectrum measured at 80 K is dominated by neutral donor-bound exciton emission (D^0X) located at 3.522 eV for the *n*-type MgZnO:N film, but by neutral acceptor-bound exciton emission (A^0X) located at 3.515 eV for the *p*-type MgZnO:N film. By fitting exciton emission intensity of temperature-dependent PL spectra, the binding energies of the D^0X and A^0X were estimated to be 32 and 43 meV, respectively. Based on the energy shift of exciton emission, the band gap of the MgZnO:N film is estimated to be 3.613 eV, which is 179 meV larger than that of ZnO. Using the Haynes rule, the acceptor energy level of the MgZnO:N film was evaluated to be about 176 meV above the valence band.

I. INTRODUCTION

Owing to a wide band gap of 3.37 eV and large exciton binding energy of 60 meV at room temperature, ZnO is considered to be a candidate material for preparation of short wavelength optoelectronic devices, such as light-emitting diode (LED) and laser diode (LD), etc.^{1,2} In the recent years, investigations on *p*-type ZnO and ZnO-based LED made a great progress. The *p*-type ZnO LEDs were prepared by single doping of I or V group elements, such as, Li, N, and P, etc., and codoping of III–V groups, such as Al–N, etc.^{3–6} Electroluminescence (EL) of ZnO *p*-*n* homojunction LEDs was also realized recently^{7–9}; however, the EL wavelengths are not in ultraviolet (UV) range but a blue or yellow light range. To obtain strong near-band-edge UV emission and even high-efficiency UV laser, it is necessary to fabricate LED and LD with

active layers composed of ZnO-based superlattices and quantum wells, which need not only fabricate high-quality *p*-type ZnO, but also develop ZnO alloys barrier materials with band gaps larger than that of ZnO. Since band gap of $Mg_xZn_{1-x}O$ alloy with wurtzite structure is larger than that of ZnO and can be tuned by changing of Mg concentration,^{10,11} $Mg_xZn_{1-x}O$ alloy is proposed to be used as candidate barrier material for fabrication of ZnO-based quantum wells or superlattices. In the recent years, much research was carried out on $Mg_xZn_{1-x}O$ alloy, and *n*-type $Mg_xZn_{1-x}O$ alloy has been produced; however, fabrication of *p*-type $Mg_xZn_{1-x}O$ alloy is still difficult. The *p*-type MgZnO alloys were only reported to be prepared by phosphor doping and N–Al codoping,^{12,13} we produced *p*-type MgZnO by using nitrogen doping followed by post annealing process.¹⁴ However, this research is focused on the fabrication and electric characteristics of *p*-type MgZnO, while investigation on the optical features and acceptor energy level state are limited.

A better understanding of the luminescence properties

^{a)}Address all correspondence to this author.

e-mail: yaobin196226@yahoo.com.cn

DOI: 10.1557/JMR.2007.0349

of MgZnO thin films would be very crucial for designing and developing LED and LD devices with active layers of ZnO-based superlattices and quantum wells. In the present work, temperature-dependent photoluminescence (PL) was studied for the *n*-type as-grown and *p*-type annealed nitrogen-doped MgZnO (MgZnO:N) alloy films grown by plasma-assisted molecular-beam epitaxy (PAMBE), and binding energies of the neutral bound excitons as well as the acceptor energy level of the *p*-type MgZnO:N were evaluated.

II. EXPERIMENTAL PROCEDURES

A MgZnO:N film was grown on *c*-plane sapphire (Al_2O_3) at 425 °C by PAMBE. Metal Zn (99.9999% in purity) and Mg (99.999% in purity) were used as Zn and Mg source. 99.99% pure NO gas was activated by an Oxford Applied Research (Oxfordshire, UK) Model HD25 r.f. (13.56 MHz) atomic source at 300 W and used as oxygen and dopant source. The details about the growth of the MgZnO films were described elsewhere.¹⁴ The structure of the film was identified by x-ray diffraction (XRD) with Cu $K_{\alpha 1}$ radiation. The thickness of the film was measured by ellipsometer to be about 200 nm. The electrical properties were detected by a Hall analyzer (Lakeshore 7707, Westerville, OH) in Van der Pauw configuration at room temperature. PL measurements were performed using a He–Cd laser with a wavelength of 325 nm as excitation source in a temperature ranging from 80–300 K.

III. EXPERIMENTAL RESULTS AND DISCUSSION

XRD measurement indicates that the as-grown MgZnO:N film consists of a single wurtzite structure with (002) preferential orientation and remains this structure after annealed for 1 h at 600 °C in an O_2 flow.¹⁴ It is believed that the Mg concentration in both films is the same due to the same diffraction peak positions in the XRD measurements. The x-ray photoelectron spectroscopy (XPS) calculation shows that about 20 at.% Zn is replaced by Mg in the as-grown MgZnO:N.¹⁴ Hall-effect measurements show that the as-grown MgZnO:N film displays *n*-type conduction with a electron concentration of $3.0 \times 10^{18} \text{ cm}^{-3}$ and a mobility of $1.10 \text{ cm}^2/\text{V s}$, but *p*-type conduction with a hole concentration of $6.1 \times 10^{17} \text{ cm}^{-3}$ and a mobility of $6.42 \text{ cm}^2/\text{V s}$ after annealed for 1 h at 600 °C in an O_2 flow. To understand this conduction transition, XPS measurement was performed for the as-grown and annealed MgZnO:N films, as shown in Fig. 1. Curve (a) in Fig. 1 shows that there are two chemical environments of $(\text{N})_{\text{O}}$ acceptor and $(\text{N}_2)_{\text{O}}$ double donors in the as-grown MgZnO:N film—located at 396.1 and 404.3 eV, respectively (the 400.0 eV peak is assigned to radiation of N 1s in C–N bond). After annealing, as shown in curve (b) of Fig. 1, the $(\text{N}_2)_{\text{O}}$ band

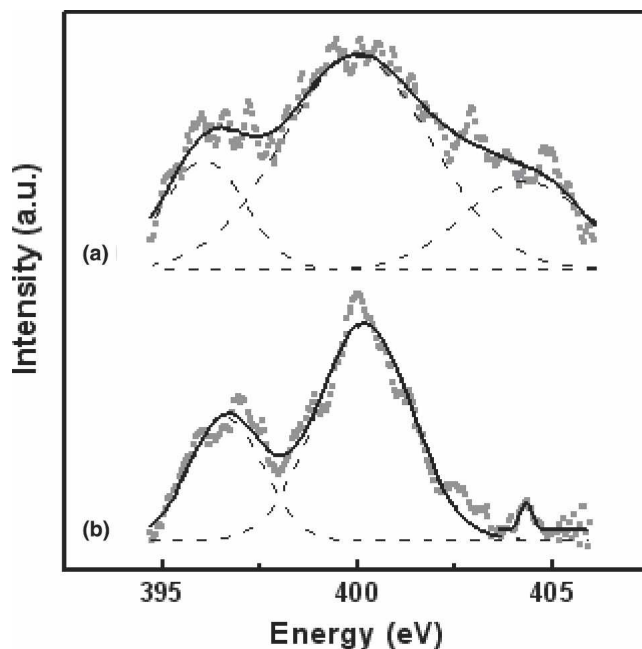


FIG. 1. N 1s peaks of x-ray photoelectron spectra of (a) as-grown and (b) annealed MgZnO:N films.

almost disappears, while $(\text{N})_{\text{O}}$ peak becomes dominant, indicating that the $(\text{N}_2)_{\text{O}}$ donors are few, while $(\text{N})_{\text{O}}$ acceptor defects become dominant defects in the MgZnO:N film. Therefore, the conduction transition from *n*-type to *p*-type for the MgZnO:N film is primary attributed to the reduce of $(\text{N}_2)_{\text{O}}$ double-donor defects after annealed.¹⁴

The temperature-dependent PL spectra of the *n*-type and *p*-type MgZnO:N films were shown in Figs. 2(a) and 2(b), respectively. At the low temperature (80 K), the

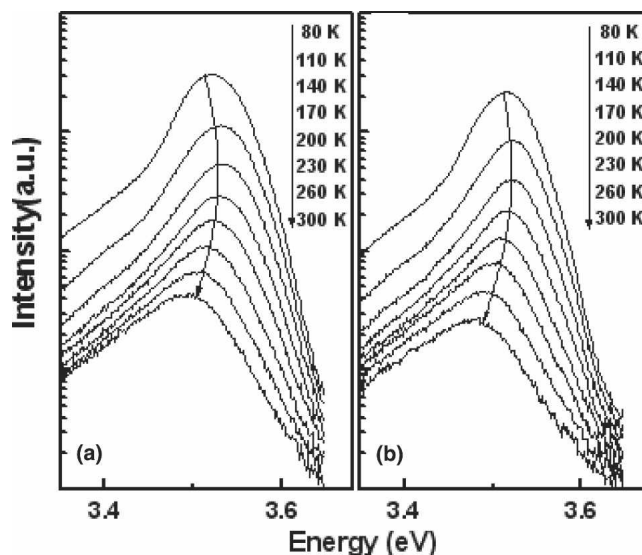


FIG. 2. Temperature dependent PL spectra of the MgZnO:N film. (a) As-grown sample with *n*-type conduction. (b) Annealed sample with *p*-type conduction.

spectrum of the *n*-type MgZnO:N film shows an emission peak centered at 3.522 eV, while that of the *p*-type MgZnO:N film exhibits an emission peak at 3.515 eV. The photon energies of the both peaks are higher than ZnO band gap due to Mg doping. According to the energy values and previous reports,¹⁵ both emissions are ascribed to the exciton-related emissions.

As the temperature increases, the PL peak positions of both films show blue shift first in a temperature ranging from 80 to about 130 K, and then red shift obviously up to 300 K. These phenomena are different from temperature-dependent band gap,¹⁶ which shows red shift with increasing temperature. To characterize the change of PL with temperature clearly, each of PL spectra recorded in the temperature range of 80–300 K was fitted with Gaussian fitting method to obtain exact photon energies and integral intensity of the PL peaks at various temperatures. The change of the photon energies with temperature is plotted in Fig. 3, indicating obvious peak position shift with temperature and a change of the shift tendency at about 130 K; the latter implies that the PL peaks do not come from one kind of emission and that the thermal quenching undergoes two different processes with a change at about 130 K. According to our previously reported literature,¹⁵ the peaks originate from two kinds of emissions. One comes from the free exciton emission, located at high-energy side and the other from the bound exciton emission, located at low-energy side.

Due to the large binding energy of bound exciton in wide gap alloy, the two PL peaks in Figs. 2(a) and 2(b) come mainly from contribution of the bound exciton emissions rather than free exciton emissions at 80 K. Compared with the peak position of the as-grown film

shown in Fig. 3, the peak position of the annealed MgZnO:N film occurs at 7 meV red shift. As described above and previously reported,¹⁴ the conduction-type transition occurs because the (N₂)_O double donor and native defect donors decreased after annealing while the N_O acceptor became the dominant defect in *p*-type annealed sample, which is confirmed by XPS and Hall measurements. In general, the binding energy of acceptor-bound exciton (A⁰X) is larger than that of donor-bound exciton (D⁰X), and the A⁰X locates at the low-energy side of the D⁰X.^{17,18} So, the red shift indicates that contribution of A⁰X emission increases after annealing, which is in agreement with the Hall and XPS measurement results mentioned above. Therefore, it can be deduced that the 3.522 eV peak should originate mainly from D⁰X emission while the 3.515 eV peak originates mainly from A⁰X emission.

During the increasing temperature process, the thermal quenching of the UV peak is attributed to the dissociation of the bound exciton to free exciton and the dissociation of the free exciton. The thermal quenching process is primarily attributed to the dissociation of the bound exciton in low-temperature range (80 K < *T* < 130 K), resulting in the peak position blue shift, but to the dissociation of the free exciton in high-temperature range (130 K < *T* < 300 K), leading to peak position red shift. In the high-temperature range, the decrease of the band gap with increasing temperature is predominant, which induces the red shift. Since the free exciton from the bound exciton dissociation becomes predominant with increasing temperature, the energy difference of the peak positions of the *n*-type and *p*-type samples decreased with increasing temperature. Due to the large binding energy of bound exciton, the bound exciton has not dissociated entirely into free exciton even at 300 K, resulting in existence of the energy difference. By fitting the peak positions, the stretched-out lines converge at about 390 K. Above this temperature, the PL peak energy approaches the free exciton position due to the dissociation of bound exciton, and the difference of peak position of both samples can be neglected. We can forecast that the difference will vanish when the PL recombination almost comes from free exciton in higher temperature.

To confirm the dissociation processes of exciton complexes, Fig. 4 illustrates the energy dispersion of PL lines with the variation of temperature in low- and high-temperature ranges. The temperature dependence of the PL intensity *I* can be expressed as

$$I = I_0 / [1 + C \exp(-E_1/kT)] \quad (1)$$

where *C* is the fitting parameter, *E*₁ is the binding energy, *k* is the Boltzmann constant, and *I*₀ is constant. The *I* is defined as integral area of an emission band. By fitting the plot of the temperature-dependent exciton emission intensity (Fig. 4) with Eq. (1), the energy for thermal

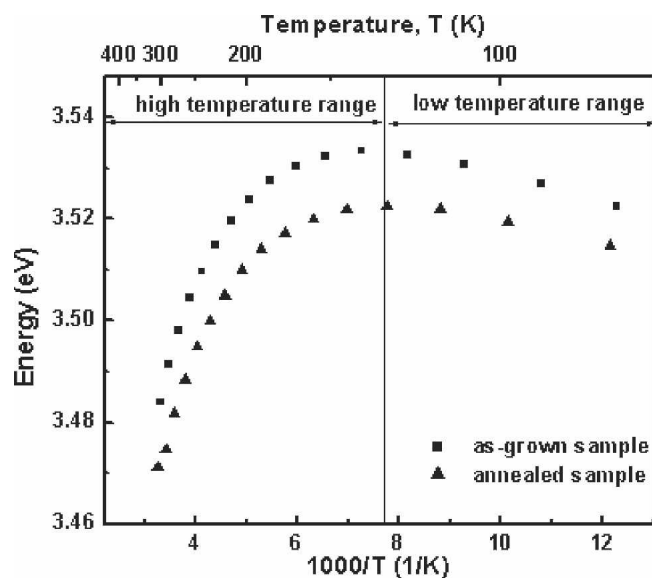


FIG. 3. Plots of the emission energies of the *n*-type (■) and *p*-type (▲) MgZnO:N as a function of measurement temperature.

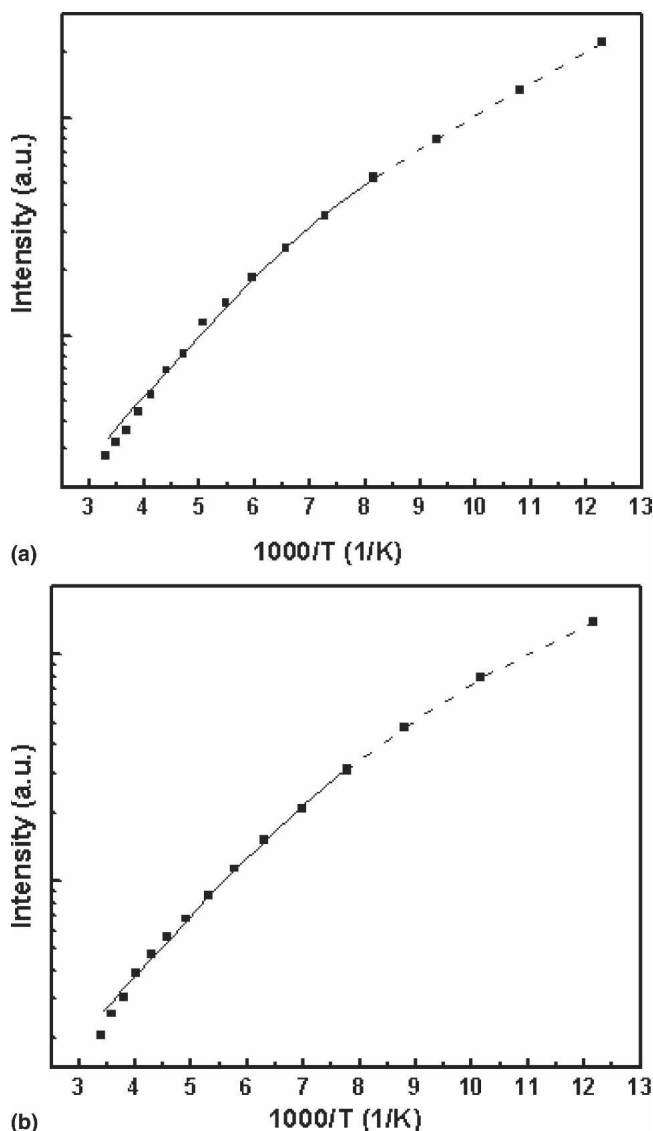


FIG. 4. Temperature dependence of the emission intensity of (a) *n*-type as-grown MgZnO:N and (b) *p*-type annealed MgZnO:N. The theoretical simulations by Eq. (1) to the experimental data points (dash line is fitted in low-temperature region, solid line is fitted in high-temperature region).

release of excitons can be obtained. In the case of *n*-type sample [Fig. 4 (a)], the binding energies are estimated to be 32.0 ± 0.1 meV in low-temperature range (dash line) and 59 ± 2 meV in high-temperature range (solid line), respectively. For the *p*-type sample [Fig. 4 (b)], the binding energies are 43.0 ± 0.1 meV (dash line) and 56 ± 2 meV (solid line), respectively. The dissociation of the free exciton is dominant in the high-temperature range. So the fitting results in high-temperature range are the binding energies of free exciton. The binding energies of the two samples are consistent with the result reported by Schmidt et al.,¹⁹ who indicate that the free exciton binding energy of MgZnO alloy film was considered to be slightly smaller than that of ZnO bulk materials (60

meV). According to the fitting results in the low-temperature range, the binding energies of the bound exciton are 32 meV for D^0X and 43 meV for A^0X , respectively. The peak of free exciton emission located at 3.374 eV with free exciton binding energy of 60 meV in ZnO, while the peak of D^0X located at 3.522 eV with donor-binding energy and free exciton binding energy of 32 and 59 meV in as-grown MgZnO:N film at 80 K. The band gap of MgZnO:N and ZnO can be calculated to be 3.613 and 3.434 eV, respectively. Namely, Mg doping causes a band gap increase of 179 meV. We can also calculate the acceptor energy level using the Haynes rule $E_{loc} = a + bE_A$, where E_{loc} is binding energy of the bound exciton, E_A is acceptor energy level, and a and b are constants. Using the values $a = -0.021$, $b = 0.244$ for ZnO material system reported by Gutowski et al.,²⁰ the N_O acceptor level in the *p*-type MgZnO:N film can be estimated to be 176 meV, larger than N_O level of 142 meV in the *p*-type N-doped ZnO.²¹

IV. CONCLUSIONS

An *n*-type MgZnO:N film was fabricated by PAMBE using radical NO as the oxygen source and nitrogen dopant, and *p*-type MgZnO:N was prepared by annealing of the as-grown MgZnO:N film for 1 h at 600 °C in an O_2 flow. The 80 K PL spectrum is dominated by D^0X peak located at 3.522 eV for the *n*-type MgZnO:N film while by A^0X peak located at 3.515 eV for *p*-type MgZnO:N film. The binding energy of the D^0X was estimated to be 32 meV, while the binding energy of the A^0X to be 43 meV. The binding energy of free exciton in the MgZnO:N film is estimated to be about 56 to 59 ± 2 meV. The band gap of the MgZnO:N film is estimated to be 3.613 eV, which is 179 meV larger than that of ZnO. Using the Haynes rule, the acceptor energy level of the *p*-type MgZnO:N film was estimated to be 176 meV above the valence band.

ACKNOWLEDGMENTS

This work is supported by the Key Project of National Natural Science Foundation of China under Grant Nos. 60336020 and 50532050, the “973” program under Grant No. 2006CB604906, the Innovation Project of Chinese Academy of Sciences, the National Natural Science Foundation of China under Grant Nos. 60429403, 60506014, 50402016, 10674133, 10647105, and 60676059.

REFERENCES

1. Z.K. Tang, G.K.L. Wong, P. Yu, M. Kawasaki, A. Ohtomo, H. Koinuma, and Y. Segawa: Room-temperature ultraviolet laser

- emission from self-assembled ZnO microcrystallite thin films. *Appl. Phys. Lett.* **72**, 3270 (1998).
2. H. Cao, J.Y. Wu, H.C. Ong, J.Y. Dai, and R.P.H. Chang: Second harmonic generation in laser ablated zinc oxide thin films. *Appl. Phys. Lett.* **73**, 572 (1998).
 3. D.C. Look, D.C. Reynolds, C.W. Litton, R.L. Jones, D.B. Eason, and G. Cantwell: Characterization of homoepitaxial *p*-type ZnO grown by molecular beam epitaxy. *Appl. Phys. Lett.* **81**, 1830 (2002).
 4. H.W. Liang, Y.M. Lu, D.Z. Shen, Y.C. Liu, J.F. Yan, C.X. Shan, B.H. Li, Z.Z. Zhang, J.Y. Zhang, and X.W. Fan: *p*-type ZnO thin films prepared by plasma molecular beam epitaxy using radical NO. *Phys. Status Solidi A* **202**, 1060 (2005).
 5. K. Kyoung-Kook, K. Hyun-Sik, H. Dae-Kue, L. Jae-Hong, and P. Seong-Ju: Realization of *p*-type ZnO thin films via phosphorus doping and thermal activation of the dopant. *Appl. Phys. Lett.* **83**, 63 (2003).
 6. T. Yamamoto and H. Katayama-Yoshida, Solution using a codoping method to unipolarity for the fabrication of *p*-type ZnO. *Jpn. J. Appl. Phys., Part 2* **38**, L166 (1999).
 7. A. Tsukazaki, T. Onuma, M. Ohtani, T. Makino, M. Sumiya, K. Ohtani, S.F. Chichibu, S. Fuke, Y. Segawa, H. Ohno, H. Koinuma, and M. Kawasaki: Repeated temperature modulation epitaxy for *p*-type doping and light-emitting diode based on ZnO. *Nat. Mater.* **4**, 42 (2005).
 8. S.J. Jiao, Z.Z. Zhang, Y.M. Lu, D.Z. Shen, B. Yao, J.Y. Zhang, B.H. Li, D.X. Zhao, X.W. Fan, and Z.K. Tang: ZnO *p-n* junction light-emitting diodes fabricated on sapphire substrates. *Appl. Phys. Lett.* **88**, 031911 (2006).
 9. W. Liu, S.L. Gu, J.D. Ye, S.M. Zhu, S.M. Liu, X. Zhou, R. Zhang, Y. Hang, and C.L. Zhang: Blue-yellow ZnO homostructural light-emitting diode realized by metalorganic chemical vapor deposition technique. *Appl. Phys. Lett.* **88**, 092101 (2006).
 10. A. Ohtomo, M. Kawasaki, T. Koida, K. Masubuchi, and H. Koinuma: Mg_xZn_{1-x}O as a II–VI widegap semiconductor alloy. *Appl. Phys. Lett.* **72**, 2466 (1998).
 11. S. Choopun, R.D. Vispute, W. Yang, R.P. Sharma, T. Venkatesan, and H. Shen: Realization of band gap above 5.0 eV in metastable cubic-phase Mg_xZn_{1-x}O alloy films. *Appl. Phys. Lett.* **80**, 1529 (2002).
 12. Y.W. Heo, Y.W. Kwon, Y. Li, S.J. Pearton, and D.P. Norton: *p*-type behavior in phosphorus-doped (Zn,Mg)O device structures. *Appl. Phys. Lett.* **84**, 3474 (2004).
 13. X. Zhang, X.M. Li, T.L. Chen, C.Y. Zhang, and W.D. Yu: *p*-type conduction in wide-gap Zn_{1-x}Mg_xO films grown by ultrasonic spray pyrolysis. *Appl. Phys. Lett.* **87**, 092101 (2005).
 14. Z.P. Wei, B. Yao, Z.Z. Zhang, Y.M. Lu, D.Z. Shen, B.H. Li, X.H. Wang, J.Y. Zhang, D.X. Zhao, X.W. Fan, and Z.K. Tang: Formation of *p*-type MgZnO by nitrogen doping. *Appl. Phys. Lett.* **89**, 102104 (2006).
 15. C-X. Wu, Y-M. Lu, D-Z. Shen, Z-P. Wei, Z-Z. Zhang, B-H. Li, J-Y. Zhang, Y-C. Liu, and X-W. Fan: Ultraviolet luminescence in Mg_{0.12}Zn_{0.88}O alloy films. *Chin. Phys. Lett.* **22**, 2655 (2005).
 16. X.T. Zhang, Y.C. Liu, Z.Z. Zhi, J.Y. Zhang, Y.M. Lu, D.Z. Shen, W. Xu, X.W. Fan, and X.G. Kong: Temperature dependence of excitonic luminescence from nanocrystalline ZnO films. *J. Lumin.* **99**, 149 (2002).
 17. D.C. Look and B. Clafin: *p*-type doping and devices based on ZnO. *Phys. Status Solidi B* **241**, 624 (2004).
 18. H. Dae-Kue, K. Hyun-Sik, L. Jae-Hong, O. Jin-Yong, Y. Jin-Ho, P. Seong-Ju, K. Kyoung-Kook, D.C. Look, and Y.S. Park: Study of the photoluminescence of phosphorus-doped *p*-type ZnO thin films grown by radio-frequency magnetron sputtering. *Appl. Phys. Lett.* **86**, 151917 (2005).
 19. R. Schmidt, B. Rheinlander, M. Schubert, D. Spemann, T. Butz, J. Lenzner, E.M. Kaidashev, M. Lorenz, A. Rahm, H.C. Semmelhack, and M. Grundmann: Dielectric functions (1 to 5 eV) of wurtzite Mg_xZn_{1-x}O ($x \leq 0.29$) thin films. *Appl. Phys. Lett.* **82**, 2260 (2003).
 20. J. Gutowski, N. Presser, and I. Broser: Acceptor-exciton complexes in ZnO: A comprehensive analysis of their electronic states by high-resolution magneto-optics and excitation spectroscopy. *Phys. Rev. B* **38**, 9746 (1988).
 21. S.J. Jiao, Y.M. Lu, D.Z. Shen, Z.Z. Zhang, B.H. Li, Zh.H. Zheng, B. Yao, J.Y. Zhang, D.X. Zhao, and X.W. Fan: Donor–acceptor pair luminescence of nitrogen doping *p*-type ZnO by plasma-assisted molecular-beam epitaxy. *J. Lumin.* **122–123**, 368 (2007).